IEEE Access
Multidisciplinary ⋮ Rapid Review ⋮ Open Access Journal

Received 28 July 2022, accepted 11 August 2022, date of publication 16 August 2022, date of current version 24 August 2022.

*Digital Object Identifier 10.1109/ACCESS.2022.3199072*

RESEARCH ARTICLE

# BugTalk: Online Prediction for the Life of Spodoptera Litura (Common Cutworm)

**LI-XIAN CHEN[1], WEN-LIANG CHEN[2], MING-YAO CHIANG[3], YI-BING LIN[1,4,5,6,7], (Fellow, IEEE), YUN-WEI LIN[8], (Member, IEEE), AND FUNG-LING NG[2]**

[1]Department of Computer Science, National Yang Ming Chiao Tung University, Hsinchu 300, Taiwan
[2]College of Biological Science and Technology, National Yang Ming Chiao Tung University, Hsinchu 300, Taiwan
[3]Applied Zoology Division, Taiwan Agricultural Research Institute, Taichung 413, Taiwan
[4]College of Humanities and Sciences, China Medical University, Taichung 406, Taiwan
[5]Miin Wu School of Computing, National Cheng Kung University, Tainan City 701, Taiwan
[6]Department of Computer Science and Information Engineering, Asia University, Taichung 413, Taiwan
[7]Research Center for Information Technology Innovation, Academia Sinica, Taipei 115, Taiwan
[8]College of Artificial Intelligence, National Yang Ming Chiao Tung University, Tainan 711, Taiwan

Corresponding author: Yi-Bing Lin (liny@nctu.edu.tw)

This work was supported in part by the Center for Open Intelligent Connectivity from the Featured Areas Research Center Program within the Framework of the Higher Education Sprout Project by the Ministry of Education, Taiwan; in part by the Ministry of Science and Technology under Grant 109-2221-E-009-087-MY2 and Grant 109-2221-E-009-089-MY2; and in part by the Ministry of Economic Affairs under Grant 107-EC-17-A-02-S5-007.

**ABSTRACT** Due to climate change, Spodoptera litura has the potential to become an increasingly severe pest because of increased habitat suitability. To support precision agriculture, it is essential to accurately predict the life cycle of Spodoptera litura, and use the information for pest control. This paper proposes BugTalk to predict the life of Spodoptera litura (Common Cutworm). Based on the Internet of Things (IoT) technology, BugTalk is a real-time prediction version of modified Insect Life Cycle Modeling software (ILCYM), an open-source software package that implements the functions used in the four models of the four life stages of Spodoptera litura. In this paper, we significantly improve the ILCYM functions and several models of the previous studies to improve the accuracy of the prediction. We develop the first real-time prediction system that can predict the number of Spodoptera litura for the farm fields in real-time. The results are compared with the measurements during 2014-2020. We extend the temperature-based ILCYM model to accommodate humidity for the larvae emergence stage, which further improves the accuracy of the model. The Mean Arctangent Absolute Percentage Error (MAAPE) between the measurements and the BugTalk prediction is 24.593%. This result has been practically utilized in farm management.

**INDEX TERMS** Internet of Things (IoT), life cycle modeling, pest control, phenology model, smart agriculture, Spodoptera litura.

## I. INTRODUCTION

Spodoptera litura (Fabr.) is omnivorous, which is harmful to grain crops, vegetables, fruits, foliage plants, and a variety of flowers [1]. This pest is a destructive pest with a wide range of hosts in tropical and subtropical Asia, Africa (Reunion), Europe (UK), the USA (Hawaii), Australia, and the Pacific islands [2]. These common cutworms endanger, for example, the young leaves of the Phalaenopsis orchid in the greenhouse so that the growth of the plant is affected. Female adults lay eggs on the back of the leaves, hatching larvae in groups to endanger the young leaves of the seedling stage or growing plants, and the epidermis remains after chewing the leaf flesh on the back of the leaves, showing transparent eating marks or holes [3]. Growing larvae lurk in planted timber or dead leaves during the day and come out to harm after dusk and early in the morning. Old mature larvae infiltrate the planted timber or soil to pupate. The damaged leaves fall on the

The associate editor coordinating the review of this manuscript and approving it for publication was Renato Ferrero.

plant timber, and many dark green granular feces can be seen on the plant material. They also endanger the flowers during the flowering period, chew on the petals, and make the flowers lose their beauty and ornamental value. The life of Spodoptera litura can be longer than 80 days [4].

(A) female adult (B) eggs (C) larva (D) pupa

**FIGURE 1.** Spodoptera litura (A) female adult (B) eggs (C) larva (D) pupa.

The adults (Fig. 1 (A)) are 15–20 mm long and the hindwings are off-white with a dark brown outer rim and spread 30–38 mm. The ratio of males and females is 1:1 [5]. Female adults begin laying eggs 1-4 days after mating, averaging 300 eggs per egg mass, which varies in size and is elongated, and covered with yellow tail hairs. Adults live from 8 to 37 days. The egg hatchability stage is 2-8 days, the larval stage is 10-56 days, and the pupal stage is 6-21 days. The egg (Fig. 1 (B)) is slightly flattened, pale yellowish-green, with radial ridges and a diameter of 0.6 mm. The larvae (Fig. 1 (C)) are 40–45 mm long and vary in color, ranging from grey-black to dark green, and are reddish-brown or yellowish-white. The pupae (Fig. 1 (D)) are 15–20 mm long and are yellow-green or pale green when pupated, later become reddish-brown and shiny, spindle-shaped, with two tail spines at the end, curved downwards [6].

Due to climate change, Spodoptera litura has the potential to become an increasingly severe pest because of increased habitat suitability. To support precision agriculture, it is essential to accurately predict the life cycle of Spodoptera litura. Such a goal can be achieved with the advent of the Internet of Things (IoT) technology to the applied biological sciences. In this paper, we use an IoT application development platform called IoTtalk to study the influence of weather conditions on the life of Spodoptera litura. Specifically, we propose an IoTtalk-based application called BugTalk to develop four stage emergence models:

**Model 1** for the oviposition stage predicts the number of eggs in the future based on the number of female adults and the temperature.

**Model 2** for the larvae emergence stage predicts the larvae population in the future based on the number of eggs, temperature, and humidity.

**Model 3** for the pupation stage predicts the number of pupae in the future based on the number of larvae and the temperature.

**Model 4** for the adult emergence stage predicts the number of future adults based on the number of pupae and the temperature.

Through these models, we predict the development time from one stage to the next stage. An open-source software package called Insect Life Cycle Modeling software (ILCYM) [7] implements the functions used in the above four models. Based on an IoT development platform called IoTtalk [8], we propose BugTalk which reuses and modifies the codes of ILCYM to enhance the accuracy of prediction. BugTalk collects the sensor data of open farm fields and predicts the number of Spodoptera litura in real-time.

The paper is organized as follows. Section II surveys the related works; Section III proposes the oviposition stage model of Spodoptera litura; Section IV proposes the larvae emergence, the pupation, and the adult emergence models and shows how to integrate these models; Section V proposes BugTalk for predicting the life period of Spodoptera litura and evaluates its performance.

## II. RELATED WORKS

Several studies used meteorological data to predict the number of adult moths in the pitchers. In [9], the authors conducted a field experiment on soybean in India. They observed the effects of weather conditions on the population of Spodoptera litura. The study showed that the weather conditions like maximum temperature, rainfall, sunshine, and wind speed were related to the number of male Spodoptera litura adults caught in the pheromone traps. The study also showed that the peak appearance times of egg masses, larvae, and adults are similar, which is around September to October. Based on the observations, the authors proposed that the number of male adults in pheromone traps can be used to show the potential of larvae attack timing and as a reference for Spodoptera litura management on soybeans. In [10], multiple and polynomial regressions are used with machine learning methods such as multi-layer perceptron neural network (MLP-NN), artificial neural network (ANN), and polynomial neural networks (PNN) to predict the moth population in the groundnut cropping system. A four-year field experiment was conducted in [11] to investigate the seasonal dynamics of Spodoptera litura. The collected data indicated that the larval population has a significant positive correlation with weather parameters such as morning humidity and temperature. The proposed model predicted the population of Spodoptera litura in castor to suggest optimal management strategies. These approaches did not provide information about the life dynamics of Spodoptera litura.

Several studies derived the relationship between the temperature of the environment and the number of adults and larvae. In [12], the authors investigated the seasonal incidence of Spodoptera litura in the greenhouse. The study indicated that maximum temperature is positively correlated with moth population, fruit infestation, and larval population of Spodoptera litura. While morning humidity had a positive correlation with moth population and fruit infestation,

evening relative humidity had a positively significant correlation with the larval population. A field experiment was conducted to study the larval population of Spodoptera litura ranging from 0.56 to 1.57 larvae/plant [13]. The experiment indicated a strong positive correlation between the larval population and temperature, and a negative correlation between the population and relative humidity. These studies did not give the dynamics of the life cycle information for Spodoptera litura.

Based on constant temperature measurements in the laboratory, the study [14] proposed a population model to predict the insect population. This model first analyzes an insect's mortality stochastically and then develops a reproduction response to temperature on a physiological time scale. The physiological age is the accumulation of the developmental rate or the senescence rate from the beginning to the present time in a life stage. This study described the conditions between the temperature response properties and physiological age to establish the validity of the model. Then several studies have been devoted to developing similar models.

In [15] a temperature-based model was proposed to study the development of Lepidoptera Carposinidae and its stage emergence. The stage emergence models were constructed using the modified Sharpe and DeMichele model and the two-parameter Weibull function. The study indicated that the development times are decreasing functions of temperature up to 32.8°C in eggs, up to 28.8°C in larvae, and up to 30.8°C in pupae. Similar observations were made in [16]. Specifically, the study showed that the overall adult survival exhibited a reverse logistic curve against the temperature. In [17], abiotic factors on Spodoptera litura were studied by decreasing temperature from 27±2°C and relative humidity from 70±5%. The results show the influence of abiotic factors like temperature and humidity on the lifecycle of Spodoptera litura which can help in the prediction of population dynamics of insect pests.

The indoor laboratory study in [18], [19] investigated the cold survival strategy of Spodoptera litura. Based on Metabolomics, the authors analyzed the metabolic features of larvae at two low temperatures: 15°C and 4°C. The results indicated that cold exposure decreases free amino acids level due to a metabolic energy shift from carbohydrate to lipid. Concurrence of food supplements and fluctuating temperatures are likely to facilitate the cold survival of larvae.

In [20], thermal reaction norms were constructed with both constant and fluctuating temperatures within the range of 15–38°C to cohorts for single-life stage measurements of Spodoptera litura, and the authors derived a temperature-based phenology model based on the measured data. This model stochastically estimates the parameter constants of the life function to examine the potential future pest status of Spodoptera litura from the SRES A1B climate change scenario for the year 2050. The results indicated that for all immature life stages, the developmental rate increases linearly with the temperature until approximately 34–36°C. The life stages were not developed when the temperature is higher than 38°C. The effects of other abiotic and biotic factors were not considered in this study. Our BugTalk proposal modifies the equations given in this related work [20] to support Models 1-4. In [21], Sharpe and DeMichele's model was modified based on Hultin's formulation to develop a biological temperature-dependent rate model, which is further enhanced in Model 2 of BugTalk to accommodate both temperature and humidity.

The above related studies [15], [16], [17], [18], [19], [20] developed and validated Models 1-4 through laboratory experiments. Their results are used in both ILCYM and BugTalk.

ILCYM implements temperature-based phenology models to understand the dynamics of insect pest populations in ecosystems. ILCYM complies with the development, mortality, and reproduction of an insect species into a phenology model. The study in [7] presented an updated version of ILCYM with a rate summation approach to simulate multidimensional age and stage-structured populations. The authors used the model and the parameters in [20] were validated by ILCYM. BugTalk reuses and modifies the codes of ILCYM to enhance the accuracy of prediction.

## III. MODEL 1: THE OVIPOSITION STAGE MODEL

In Sections III and IV, we described the models to be accommodated in BugTalk. Model 1 describes the life dynamics of Spodoptera litura at the oviposition stage by predicting the number of eggs $M_1\,(N_F, \boldsymbol{T_n})$ in the $n$th day based on the number of female adults $N_F$ at day 1 and the temperature set $\boldsymbol{T_n} = \bigcup_{i=1}^{n} \{T_1^i, \ldots, T_{24}^i\}$, where $T_j^i$ is the temperature of the $j$th hour of day $i$ for $1 \le i \le n$, $1 \le j \le 24$. We will illustrate the temperature histogram $\boldsymbol{T_n}$ for the farm we observed in Taiwan during 2014-2020 in Fig. 9 of Section V.

The equation $M_1\,(N_F, \boldsymbol{T_n})$ for Model 1 is expressed as

$$\boldsymbol{M_1}\,(\boldsymbol{N_F}, \boldsymbol{T_n}) = \begin{cases} 0 & n = 1 \\ N_F M_{1,1}\left(\boldsymbol{T_{n-1}}\right) & \\ \quad \times \left[M_{1,2}\left(\boldsymbol{T_n}\right) - M_{1,2}\left(\boldsymbol{T_{n-1}}\right)\right] & \\ \quad \times \left[1 - M_{1,3}(\boldsymbol{T_n})\right] & n > 1 \end{cases} \tag{1}$$

where $N_F$ is the number of female adults observed on day 1, $M_{1,1}\,(\boldsymbol{T_n})$ is the number of eggs produced by a female adult in its life under the temperature condition $\boldsymbol{T_n}$, $M_{1,2}\,(\boldsymbol{T_n})$ is the cumulative oviposition rate at day $n$ under condition $\boldsymbol{T_n}$, and $M_{1,3}\,(\boldsymbol{T_n})$ is the probability that the female adult is dead at day $n$ under $\boldsymbol{T_n}$.

In Eq. (1), $M_{1,1}\,(\boldsymbol{T_n})$ is derived from the 4th equation $\bar{f}_4$ described in [20], which was obtained from the Exponential curve fitting of experimental data. This function gives the total number of eggs produced by a female adult during her life span under a constant temperature $T_4$:

$$\bar{f}_4\,(T_4) = e^{\left(-13.30 + 1.59T_4 - 0.03{T_4}^2\right)} \tag{2}$$

Fig. 2 plots $\bar{f}_4(T_4)$ against $T_4$ (the green curve with triangle marks) based on the above equation. We found that the parameter constants in that equation are not precise enough, and its errors from the correct values (the blue circles) may be significant. Based on the experiments in [20], we modify $\bar{f}_4(T_4)$ by using more accurate parameter constants to generate a precise equation listed below (the red curve with square marks in Fig. 2):

$$f_4(T_4) = e^{(-13.30771+1.59219T_4-0.03098T_4^2)} \tag{3}$$

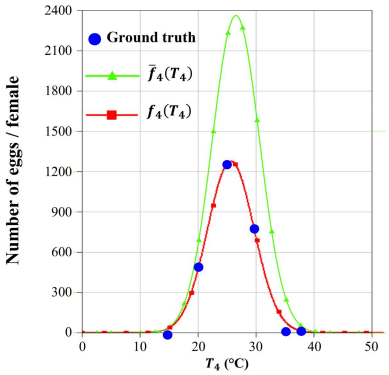


**FIGURE 2.** The $\bar{f}_4(T_4)$ and $f_4(T_4)$ curves.

In Model 1, Eq. (3) under fixed temperature $T_4$ is modified to accommodate variable temperature conditions $\boldsymbol{T_n}$ as

$$M_{1,1}(\boldsymbol{T_n}) = \left(\frac{1}{24}\right)\sum_{j=1}^{24} e^{-13.30771+1.59219T_j^n-0.03098\left(T_j^n\right)^2} \tag{4}$$

In Eq. (1), $M_{1,2}(\boldsymbol{T_n})$ is derived from the second equation $f_{2,S}$ and the 5th equation $f_5$ described in [20]. Equation $f_{2,S}$ implements a modified Sharpe and DeMichele model, which gives the immature development and adult senescence rates in Stage $S$ of Spodoptera litura (where $S = F$ for the oviposition stage, $S = E$ for the larvae emergence stage, $S = L$ for the pupation stage, and $S = P$ for the adult emergence stage) at constant temperature $T_2$:

$$f_{2,S}(T_2) = \frac{\rho_S\left(\frac{T_2}{T_{S,o}}\right)e^{\left[\left(\frac{\theta_{S,a}}{R}\right)\left(\frac{1}{T_{S,o}}-\frac{1}{T_2}\right)\right]}}{1+e^{\left[\left(\frac{\theta_{S,h}}{R}\right)\left(\frac{1}{T_{S,h}}-\frac{1}{T_2}\right)\right]}} \tag{5}$$

where at the life stage $S$, $R = 1.987$ cal/(degree mol) is the universal gas constant, $\rho_S$ is the developmental rate

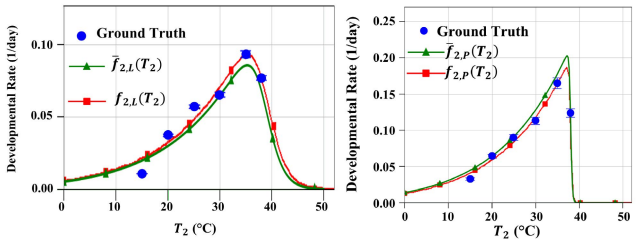


(A) $S = L$ (B) $S = P$

**FIGURE 3.** Comparing $\bar{f}_{2,S}(T_2)$ and $f_{2,S}(T_2)$. (A) $S = L$ (B) $S = P$.

at the optimum temperature $T_{S,o}$(K) assuming no enzyme inactivation, $T_{S,h}$ is the high temperature at which enzyme is half active, $\theta_{S,a}$ is the enthalpy of activation of reaction catalyzed by the enzyme (cal/mol), and $\theta_{S,h}$ is the change in enthalpy at high temperature (cal/mol). Table 3 in [20] was used to provide the parameter constants for Eq. (5), which is misleading. Let $\bar{f}_{2,S}(T_2)$ be the results using the misleading parameter values in [20]. Fig. 3 plots $\bar{f}_{2,L}(T_2)$ and $\bar{f}_{2,P}(T_2)$ (the green curves with triangle marks). The errors between them and ground truth values (the blue dots) cannot be ignored. We list the correct values in Table 1. The correct $f_{2,L}(T_2)$ and $f_{2,P}(T_2)$ values (the red curves with rectangle marks) are consistent with the ground truth values in Fig. 3.

**TABLE 1.** Parameters for $f_{2,S}$ (for $S = E, L, P, F$).

| Stage | $\rho_S$ | $T_{S,o}$ | $\theta_{S,a}$ | $\theta_{S,h}$ | $T_{S,h}$ |
|---|---|---|---|---|---|
| Egg | 0.29 | 297.65 | 19159.01 | 78167.42 | 309.34 |
| Larva | 0.64 | 335.99 | 12972.92 | 148677.5 | 311.65 |
| Pupa | 0.682 | 331.801 | 11602.076 | 905600.212 | 311.194 |
| Female | 1.058 | 296.802 | 59142.847 | 54815.552 | 290.217 |

From Table 1, Eq. (5) without considering humidity $\boldsymbol{H_n}$ is modified as $f^*_{2,F}(\boldsymbol{T_n}, \boldsymbol{H_n} = \boldsymbol{NIL}, i)$ to capture the temperature dynamics of the $i$th day ($1 \le i \le n$) using Table 1. Eq. (6), as shown at the bottom of the page, can be denoted as $f^*_{2,S}(\boldsymbol{T_n}, \boldsymbol{NIL}, i)$ for other stage $S$ by using different parameter constants in Table 1. Note that humidity is only considered when $S = E$ in this paper. The details will be described later in Eq. (15).

Based on Eq. (6), the physiological age of female adult on the $n$th day with the temperature condition $\boldsymbol{T_n}$ can be

$$\begin{aligned} f^*_{2,F}(\boldsymbol{T_n}, \boldsymbol{NIL}, i) &= f^*_{2,S}(\boldsymbol{T_n}, \boldsymbol{NIL}, i) \\ &= \left(\frac{1}{24}\right)\sum_{j=1}^{24} \frac{1.058\left(\frac{T_j^i+273.15}{296.802}\right)e^{\left[\left(\frac{59142.847}{1.987}\right)\left(\frac{1}{296.802}-\frac{1}{T_j^i+273.15}\right)\right]}}{1+e^{\left[\left(\frac{54815.552}{1.987}\right)\left(\frac{1}{290.217}-\frac{1}{T_j^i+273.15}\right)\right]}} \end{aligned} \tag{6}$$

expressed as follows:

$$F_{2,F}\left(\boldsymbol{T_n}, \boldsymbol{NIL}\right) = \begin{cases} 0 & n = 1 \\ \sum_{i=1}^{n} f^*_{2,F}\left(\boldsymbol{T_n}, \boldsymbol{NIL}, i\right) & n > 1 \end{cases} \quad (7)$$

Eq. (8) was obtained from Gamma curve fitting of experiment data. This function gives the cumulative oviposition rate at the $i_5$th day of the oviposition stage:

$$f_5\left(i_5\right) = \int_{x=0}^{i_5} \left[\frac{x^{4.99} e^{-10.32x}}{(1/10.32)^{5.99}\Gamma\left(5.99\right)}\right] dx \quad (8)$$

Substitute Eq. (7) into to Eq. (8) to yield

$$M_{1,2}\left(\boldsymbol{T_n}\right) = \int_{x=0}^{F_{2,F}\left(\boldsymbol{T_n}, \boldsymbol{NIL}\right)} \left[\frac{x^{4.99} e^{-10.32x}}{(1/10.32)^{5.99}\Gamma\left(5.99\right)}\right] dx \quad (9)$$

In Eq. (1), $M_{1,3}\left(\boldsymbol{T_n}\right)$ is derived from the first equation $f_{1,S}$ described in [20], which represents the probability to complete the development of stage $S$ on the $i_1$th day at the constant temperature $T_1$:

$$f_{1,S}\left(T_1, i_1\right) = \frac{1}{1 + e^{-[a_S(T_1) + b_S\ ln(i_1)]}} \quad (10)$$

where the values of the parameter constants $a_S$ and $b_S$ are listed in Table 2.

**TABLE 2. Parameters for $f_{1,S}$ (for $S = E, L, P, F$).**

| Stage | $a_S$ (15 °C) | $a_S$ (20 °C) | $a_S$ (25 °C) | $a_S$ (30 °C) | $a_S$ (35 °C) | $a_S$ (38 °C) | $b_S$ |
|---|---|---|---|---|---|---|---|
| Egg | -26.71 | -15.94 | -13.46 | -6.93 | -5.91 | -9.38 | 10.51 |
| Larva | -148.20 | -107.52 | -93.81 | -89.49 | -77.69 | -85.21 | 32.76 |
| Pupa | -58.53 | -47.33 | -41.45 | -37.56 | -31.06 | -38.06 | 17.23 |
| Female | -44.65 | -33.837 | -27.12 | -25.87 | -23.42 | -22.158 | 13.36 |

For Model 1, $b_F = 13.36$ and $M_{1,3}\left(\boldsymbol{T_n}\right)$ is supposed to integrate Eqs. (7) and (10). Unfortunately, we cannot accommodate Eq. (7) in Eq. (10) because the value for $a_F$ changes as temperatures $\boldsymbol{T_n}$ varies. Therefore, we ignore the $a_F$ parameter and replace $i_1$ by Eq. (7) as follows:

$$\begin{aligned} M_{1,3}\left(\boldsymbol{T_n}\right) &= \frac{1}{1 + e^{-b_F\ ln\left(F_{2,F}\left(\boldsymbol{T_n}, \boldsymbol{NIL}\right)\right)}} \\ &= \frac{1}{1 + e^{-13.36\ ln\left(F_{2,F}\left(\boldsymbol{T_n}, \boldsymbol{NIL}\right)\right)}} \end{aligned} \quad (11)$$

Fig. 4 shows that Eq. (10) and Eq. (11) agree with each other. The largest discrepancy occurs at $T_1$ =15°C, which is 23%. As illustrated in Fig. 9, most temperature values observed in our study are higher than 25°C, and it is appropriate to use Eq. (11) to replace Eq. (10) for non-fixed temperature scenarios.

The output value of $M_1\left(N_F, \boldsymbol{T_n}\right)$ is compared with the output of the corresponding ILCYM function for validation. ILCYM simulates the life stages of Spodoptera litura individually. In the oviposition stage, two random values are generated to represent the ability to oviposit and survive for each individual. Daily survival rate is calculated by $\left[1 - M_{1,3}\left(\boldsymbol{T_n}\right)\right]$. If the random value of survival is greater

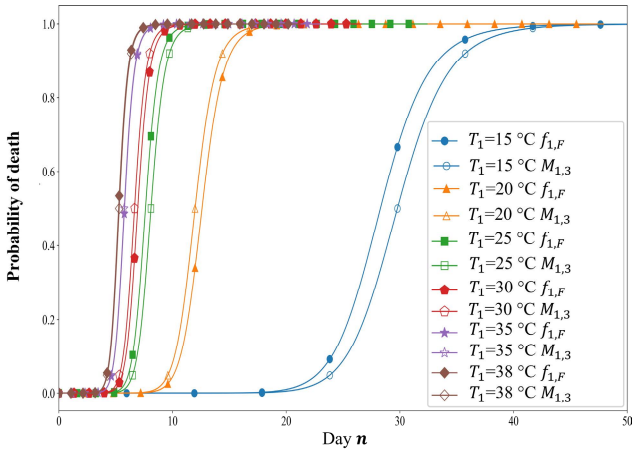


**FIGURE 4. Comparison between $f_{1,F}\left(T_1, n\right)$ and $M_{1,3}\left(T_n\right)$.**

than the survival rate on day $n$, the individual is considered dead on that day. If the individual survives at day $n$, the laying eggs of the individual on day $n$ is calculated in ILCYM by the following steps: First, the total eggs the individual can lay is calculated by $M_{1,1}\left(\boldsymbol{T_{n-1}}\right)$ and the random value of oviposition. The random value is substituted into an inverse cumulative density function (ICDF) of the normal distribution. The mean value of the distribution is $M_{1,1}\left(\boldsymbol{T_{n-1}}\right)$ and the standard deviation is $0.3 \times M_{1,1}\left(\boldsymbol{T_{n-1}}\right)$. The output of ICDF is considered as the total oviposition of the individual. By using ICDF, the total oviposition of each individual follows the normal distribution. The proportion of eggs laying by the individual on day $n$ is then calculated as $\left[M_{1,2}\left(\boldsymbol{T_n}\right) - M_{1,2}\left(\boldsymbol{T_{n-1}}\right)\right]$. Finally, the number of eggs laying on day $n$ is the product of the total oviposition value and the proportion of eggs laying.

The default number of execution times of ILCYM is 4, which is too small to obtain the converged average output. Fig. 5 shows the Mean Arctangent Absolute Percentage Error (MAAPE; which is expressed in Eq. (24) later) between Model 1 (Eq. (1)) and the ILCYM simulation (the circle curve). The curve indicates that the ILCYM converges to Eq. (1) when it is executed one million times. The figure also plots the MAAPE between Eq. (23) and ILCYM simulation (the triangle curve; details of Eq. (23) will be elaborated later). The curve indicates that the ILCYM converges to Eq. (23) when it is executed one billion times. Therefore, the default number of execution times of ILCYM is too small for its simulation.

## IV. MODELS 2–4

This section elaborates on Models 2-4 and shows how to integrate Models 1-4 to generate the final result.

### A. MODEL 2: THE LARVAE EMERGENCE STAGE

Model 2 describes the larvae emergence stage of Spodoptera litura by predicting the larvae population $M_2\left(N_E, \boldsymbol{T_n}, \boldsymbol{H_n}\right)$ in the $n$th day based on the number of eggs $N_E$ at day 1,

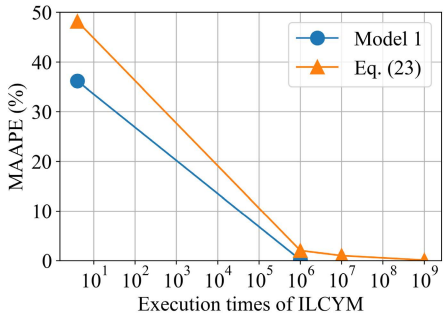


**FIGURE 5.** Comparison between the BugTalk models and the ILCYM simulation.

the temperature set $\boldsymbol{T_n}$ and the humidity set $\boldsymbol{H_n} = \cup_{i=1}^{n} \{H_1^i, \ldots, H_{24}^i\}$, where $H_j^i$ is the humidity of the $j$th hour of the day $i$ for $1 \le i \le n, 1 \le j \le 24$. Fig. 9 illustrates the relative humidity histogram for the farm we observed in Taiwan during 2014-2020. The equation for Model 2 is expressed as

$$M_2(N_E, \boldsymbol{T_n}, \boldsymbol{H_n}) = \begin{cases} N_E \left[1 - M_{2,1}(\boldsymbol{T_n}, 1)\right]^{f^*_{2,E}(\boldsymbol{T_n}, \boldsymbol{H_n}, 1)} \\ \quad \times \left[M_{2,2}(\boldsymbol{T_n}, \boldsymbol{H_n}) - 0\right] & n = 1 \\ N_E \left\{\prod_{i=1}^{n} \left[1 - M_{2,1}(\boldsymbol{T_n}, i)\right]^{f^*_{2,E}(\boldsymbol{T_n}, \boldsymbol{H_n}, i)}\right\} \\ \quad \times \left[M_{2,2}(\boldsymbol{T_n}, \boldsymbol{H_n}) - M_{2,2}(\boldsymbol{T_{n-1}}, \boldsymbol{H_{n-1}})\right] & n > 1 \end{cases} \tag{12}$$

where $N_E$ is the number of eggs observed on day 1, $M_{2,1}(\boldsymbol{T_n}, i)$ is the mortality rate of the $i$th day in the larvae emergence stage of Spodoptera litura under the temperature condition $\boldsymbol{T_n}$, $M_{2,2}(\boldsymbol{T_n}, \boldsymbol{H_n})$ is the probability that the larvae emergence stage of an egg ends at the $n$th day and it survives under condition $\boldsymbol{T_n}$ and $\boldsymbol{H_n}$. $f^*_{2,E}(\boldsymbol{T_n}, \boldsymbol{H_n}, i)$ is the development rate of the $i$th day in the larvae emergence stage of Spodoptera litura under condition $\boldsymbol{T_n}$ and $\boldsymbol{H_n}$. Note that ILCYM uses an equation similar to Eq. (12) without the humidity factor.

In Eq. (12), $M_{2,1}(\boldsymbol{T_n}, i)$ is derived from the third equation $f_{3,S}(T_3)$ in [20] based on the Wang model, which gives the mortality rate in immature life stage $S$ of Spodoptera litura at constant temperature $T_3$:

$$f_{3,S}(T_3) = 1 - e^{-d_S \left[1 + e^{-\left(\frac{T_3 - T_{S,opt}}{c_S}\right)}\right]\left[1 + e^{-\left(\frac{T_{S,opt} - T_3}{c_S}\right)}\right]} \tag{13}$$

where $T_{S,opt}$ is optimum temperature (°C) for cohort survival, and both $c_S$ and $d_S$ are fitting constants. Table 4 in [20] provides the parameter values for $f_{3,S}(T_3)$, which is misleading. Let $\bar{f}_{3,S}(T_3)$ be the equation for $f_{3,S}(T_3)$ by using the parameter constants listed in the misleading table. Fig. 6 plots $\bar{f}_{3,L}(T_3)$ (see the green curve with triangle marks). As can be seen, the error between $\bar{f}_{3,L}(T_3)$ and ground truth (the blue dots) is not negligible, and $f_{3,L}(T_3)$ fits ground truth well.

We provide the correct parameter constants in Table 3. With these correct values, we plot $f_{3,L}(T_3)$ in Fig. 6

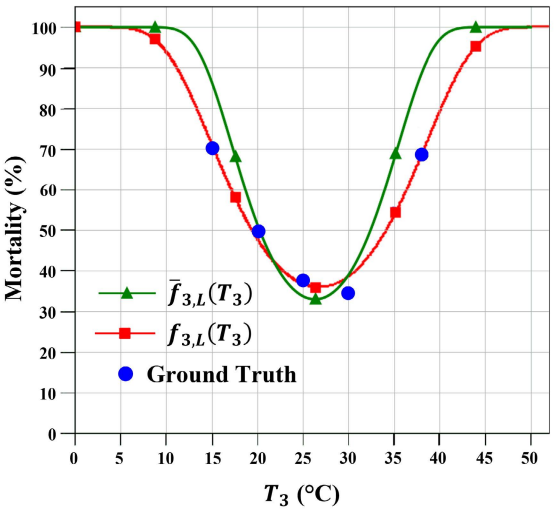


**FIGURE 6.** Comparing $f_{3,L}(T_3)$ and $\bar{f}_{3,L}(T_3)$.

**TABLE 3.** Parameters for $f_{3,S}(T_3)$ (for $S = E, L, P$).

| Stage | $T_{S,opt}$ | $c_S$ | $d_S$ |
|---|---|---|---|
| Egg | 27.012 | 3.305 | 0.025 |
| Larva | 26.800 | 5.306 | 0.111 |
| Pupa | 28.547 | 1.667 | 0.009 |

(the red curve with rectangle marks), which is consistent with ground truth. Model 2 modifies Eq. (13) to accommodate the temperature dynamics $\boldsymbol{T_n}$ as follows:

$$\begin{aligned} M_{2,1}(\boldsymbol{T_n}, i) &= 1 - \left(\frac{1}{24}\right) \sum_{j=1}^{24} e^{-d_E \left[1 + e^{-\left(\frac{T_j^i - T_{E,opt}}{c_E}\right)}\right]\left[1 + e^{-\left(\frac{T_{E,opt} - T_j^i}{c_E}\right)}\right]} \\ &= 1 - \left(\frac{1}{24}\right) \sum_{j=1}^{24} e^{-0.025 \left[1 + e^{-\left(\frac{T_j^i - 27.012}{3.305}\right)}\right]\left[1 + e^{-\left(\frac{27.012 - T_j^i}{3.305}\right)}\right]} \end{aligned} \tag{14}$$

In Eq. (12), $M_{2,2}(\boldsymbol{T_n}, \boldsymbol{H_n})$ is derived from the first equation $f_{1,S}$ described in [20] and Eq. (5), where $S = E$. We conducted experiments to collect the data for the immature development of the larvae emergence stage with various temperature and humidity conditions. Through quadrate Polynomial curve fitting (with $R^2 = 0.724$), we obtain equation $f^*_{2,E}(\boldsymbol{T_n}, \boldsymbol{H_n}, i)$ that considers both $\boldsymbol{T_n}$ and $\boldsymbol{H_n}$:

$$f^*_{2,E}(\boldsymbol{T_n}, \boldsymbol{H_n}, i) = \left(\frac{1}{24}\right) \sum_{j=1}^{24} \left[\left(8.08972 \times 10^{-5}\right)\left(H_j^i\right)^4 + \left(5.67844 \times 10^{-4}\right)\right.$$

$$\times \left(T_j^i\right)\left(H_j^i\right)^3 - \left(1.32586 \times 10^{-4}\right)\left(T_j^i\right)^2\left(H_j^i\right)^2 + \left(4.21357 \times 10^{-4}\right)\left(T_j^i\right)^3\left(H_j^i\right) + \left(3.58568 \times 10^{-4}\right) \times \left(T_j^i\right)^4 - \left(3.92490 \times 10^{-2}\right)\left(H_j^i\right)^3 - \left(1.21357 \times 10^{-1}\right) \times \left(T_j^i\right)\left(H_j^i\right)^2 - \left(1.38390 \times 10^{-2}\right)\left(T_j^i\right)^2\left(H_j^i\right) - \left(6.97315 \times 10^{-2}\right)\left(T_j^i\right)^3 + 6.00090\left(H_j^i\right)^2 + 9.48787\left(T_j^i\right)\left(H_j^i\right) + 3.29456\left(T_j^i\right)^2 - 381.47516H - 295.21231\left(T_j^i\right) + 9037.42900\Big]^{-1} \quad (15)$$

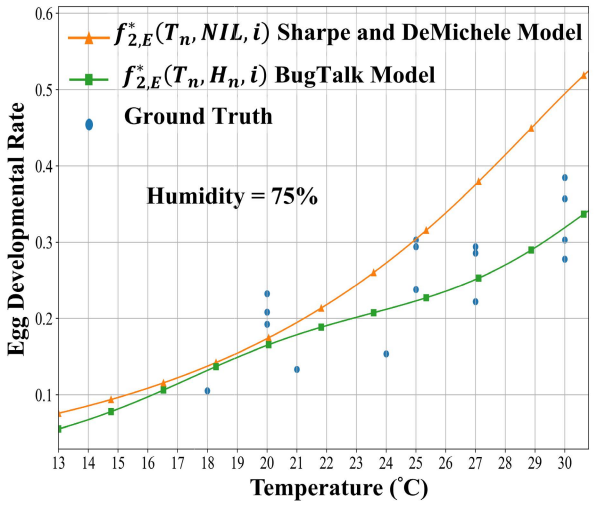


**FIGURE 7.** Comparing $f^*_{2,E}(\boldsymbol{T_n}, \boldsymbol{NIL}, i)$ and $f^*_{2,E}(\boldsymbol{T_n}, \boldsymbol{H_n}, i)$.

As an example, Fig. 7 compares $f^*_{2,E}(\boldsymbol{T_n}, \boldsymbol{NIL}, i)$ and $f^*_{2,E}(\boldsymbol{T_n}, \boldsymbol{H_n}, i)$ when the relative humidity $H_j^i$ is 75% and the temperature $T_j^i$ fixed at different temperature for $i \geq 1, 1 \leq j \leq 24$. For the range of $\boldsymbol{H_n}$ considered in this paper, our experiments indicate that the error for $f^*_{2,E}(\boldsymbol{T_n}, \boldsymbol{NIL}, i)$ is 24.42% and the error for $f^*_{2,E}(\boldsymbol{T_n}, \boldsymbol{H_n}, i)$ is 17.04%. Therefore, by considering the dynamics of the relative humidity, BugTalk improves the prediction accuracy by 30%. From Eq. (15), Model 2 uses the following equation to calculate the physiological age of eggs and produce the $M_{2,2}$ model:

$$F_{2,E}(\boldsymbol{T_n}, \boldsymbol{H_n}) = \frac{1}{2} f^*_{2,E}(\boldsymbol{T_n}, \boldsymbol{H_n}, 1) + \sum_{i=2}^{n} f^*_{2,E}(\boldsymbol{T_n}, \boldsymbol{H_n}, i) \quad (16)$$

Similar to how we derive Eq. (11), from Table 2, we substitute $F_{2,E}(\boldsymbol{T_n}, \boldsymbol{H_n})$ in the modified $f_{1,E}$ to obtain:

$$M_{2,2}(\boldsymbol{T_n}, \boldsymbol{H_n}) = \frac{1}{1 + e^{-b_E \ ln\left(F_{2,E}(\boldsymbol{T_n}, \boldsymbol{H_n})\right)}} = \frac{1}{1 + e^{-10.51 \ ln\left(F_{2,E}(\boldsymbol{T_n}, \boldsymbol{H_n})\right)}} \quad (17)$$

### B. MODELS 3, 4 AND INTEGRATION

Model 3 describes the life of Spodoptera litura at the pupation stage by predicting the number of pupae $M_3(N_L, \boldsymbol{T_n})$ in the $n$th day based on the number of larvae $N_L$ at day 1 and the temperature set $\boldsymbol{T_n}$. Similar to $M_2(N_E, \boldsymbol{T_n}, \boldsymbol{H_n})$, we have

$$M_3(N_L, \boldsymbol{T_n}) = \begin{cases} 0 & n = 1 \\ N_L \left\{ \prod_{i=2}^{n} \left[1 - M_{3,1}(\boldsymbol{T_n}, i)\right]^{f^*_{2,L}(\boldsymbol{T_n}, \boldsymbol{NIL}, i)} \right\} & \\ \quad \times \left[M_{3,2}(\boldsymbol{T_n}) - M_{3,2}(\boldsymbol{T_{n-1}})\right] & n > 1 \end{cases} \quad (18)$$

where $N_L$ is the number of larvae observed on day 1, $M_{3,1}(\boldsymbol{T_n}, i)$ is the same as $M_{2,1}(\boldsymbol{T_n}, i)$ except that $S = L$ in Table 3. $M_{3,2}(\boldsymbol{T_n})$ is the same as $M_{2,2}(\boldsymbol{T_n}, \boldsymbol{NIL})$ except that $S = L$ in Table 2, and $f^*_{2,L}(\boldsymbol{T_n}, \boldsymbol{NIL}, i)$ is same as $f^*_{2,E}(\boldsymbol{T_n}, \boldsymbol{NIL}, i)$ except that $S = L$ in Table 1.

Model 4 describes the life dynamics of Spodoptera litura at the adult emergence stage by predicting the number of future adults $M_4(N_P, \boldsymbol{T_n})$ based on the number of pupae $N_P$ and the temperature $\boldsymbol{T_n}$:

$$M_4(N_P, \boldsymbol{T_n}) = \begin{cases} 0 & n = 1 \\ N_P \left\{ \prod_{i=2}^{n} \left[1 - M_{4,1}(\boldsymbol{T_n}, i)\right]^{f^*_{2,P}(\boldsymbol{T_n}, \boldsymbol{NIL}, i)} \right\} & \\ \quad \times \left[M_{4,2}(\boldsymbol{T_n}) - M_{4,2}(\boldsymbol{T_{n-1}})\right] & n > 1 \end{cases} \quad (19)$$

where $N_P$ is the number of pupae observed on day 1, $M_{4,1}(\boldsymbol{T_n}, i)$ is the same as $M_{3,1}(\boldsymbol{T_n}, i)$ except that $S = P$ in Table 3. $M_{4,2}(\boldsymbol{T_n})$ is the same as $M_{3,2}(\boldsymbol{T_n})$ except that $S = P$ in Table 2, and $f^*_{2,P}(\boldsymbol{T_n}, \boldsymbol{NIL}, i)$ is same as $f^*_{2,L}(\boldsymbol{T_n}, \boldsymbol{NIL}, i)$ except that $S = P$ in Table 1.

By integrating Eqs. (1), (12), (18) and (19), Eq. (23) answers the following question: If we observe $N_F$ female adults at day 1, then under the weather conditions $\boldsymbol{T_n}$ and $\boldsymbol{H_n}$, what is the number $N_A(n)$ of the adults at the $n$th days. Let $\boldsymbol{T_{n_1:n_2}} = \cup_{i=n_1}^{n_2} \{T_1^i, \ldots, T_{24}^i\}$ and $\boldsymbol{H_{n_1:n_2}} = \cup_{i=n_1}^{n_2} \{H_1^i, \ldots, H_{24}^i\}$. From Eq. (1), the eggs produced at the $n_1$th day is $N_E(n_1) = M_1\left(N_F, \boldsymbol{T_{1:n_1}}\right)$. From Eq. (12), the number of larvae produced at the $n_2$th day ($n_2 \geq 1$) is

$$N_L(n_2) = \sum_{n_1=1}^{n_2} M_2\left(N_E(n_1), \boldsymbol{T_{n_1:n_2}}, \boldsymbol{H_{n_1:n_2}}\right) \quad (20)$$

Eq. (20) accumulates all larvae produced at day $n_2$ where their eggs were produced at day $n_1$ for $1 \leq n_1 \leq n_2$. In this case, the temperature and the humidity measures from the $n_1$th day to the $n_2$th day are considered. Similarly, from Eqs. (18) and (20), the number of pupae produced at the $n_3$th day ($n_3 \geq 1$) is

$$N_P(n_3) = \sum_{n_2=1}^{n_3} M_3\left(N_L(n_2), \boldsymbol{T_{n_2:n_3}}\right) \quad (21)$$

From Eqs. (19) and (21), the number of adults produced at the $n$th day ($n \geq 1$) is

$$N_A(n) = \sum_{n_3=1}^{n} M_4\left(N_P(n_3), \boldsymbol{T_{n_3:n}}\right) \quad (22)$$

Therefore, from Eqs. (1), (20), (21) and (22), we have

$$N_A(n) = \sum_{n_3=1}^{n} M_4 \left( \sum_{n_2=1}^{n_3} M_3 \left( \sum_{n_1=1}^{n_2} M_2 \left( M_1 \left( N_F, \boldsymbol{T}_{\boldsymbol{1:n_1}} \right), \boldsymbol{T}_{\boldsymbol{n_1:n_2}}, \boldsymbol{H}_{\boldsymbol{n_1:n_2}} \right), \boldsymbol{T}_{\boldsymbol{n_2:n_3}} \right), \boldsymbol{T}_{\boldsymbol{n_3:n}} \right) \quad (23)$$

## V. BUGTALK AND ITS PERFORMANCE

In BugTalk, the number $N_F$ of female adults is measured from both the pheromone traps of IoTtalk (Fig. 8 (1)) and the dataset provided by the Taiwan Agricultural Research Institute (TARI). The TARI dataset is collected from 57 farm fields in Taiwan, where every farm field was deployed with 8 pheromone traps. The data were collected from May to November during 2014-2020. Sex pheromone is used in a trap to attract male adults. The numbers of male adults captured in the traps were recorded every 10 days. Since the ratio of female and male adults is 1:1, the numbers recorded in the dataset are used as the $N_F$ variable. The hourly temperature $\boldsymbol{T_n}$ and the humidity $\boldsymbol{H_n}$ are obtained from both the micro weather stations (Fig. 8 (2)) and the datasets of Central Weather Bureau (CWB) in Taiwan. Temperature and Humidity data counts for the observed farm fields in Taiwan during 2014-2020 are illustrated in Fig. 9. The average temperature is 25.97°C with a standard deviation of 3.99; the average relative humidity is 80.42% with a standard deviation of 5.79. The sensor values used in BugTalk are displayed in the web browser (Fig. 8 (3)) of any computers or mobile devices.

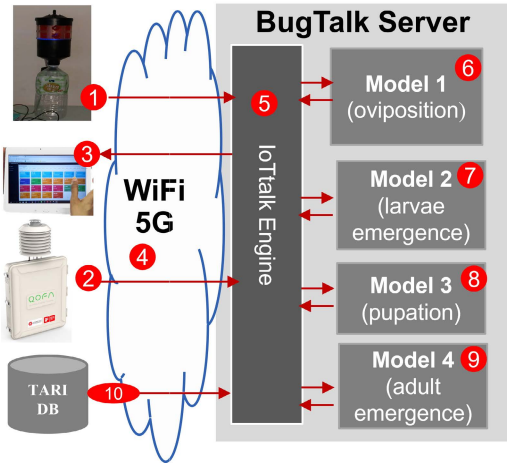


**FIGURE 8.** The BugTalk architecture.

The core of the BugTalk server is the IoTtalk engine [8], which is responsible for interaction with the IoT devices. Through wireline, Bluetooth, WiFi, or 5G (Fig. 8 (4)) the physical IoT devices are physically connected to the BugTalk server (see links (1)-(5), (2)-(5), and (3)-(5) in Fig. 8).

Besides physical IoT devices, IoTtalk can also manage cyber IoT devices. Models 1-4 (Fig. 8 (6)-(9)) are implemented as "cyber" IoT devices driven by the IoTtalk

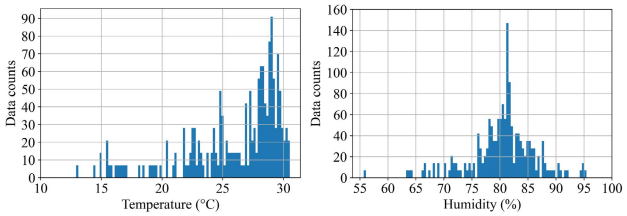


**FIGURE 9.** (A) Temperature and (B) Humidity data observed from the farm fields in Taiwan during 2014-2020.

engine [8], [22]. These models are represented as icons in the IoTtalk web-based graphical user interface (GUI), and can be easily connected to real pheromone traps and the micro weather stations through the GUI without writing any computer codes. Configuring the BugTalk application can be done through any computing device with the browser like the smartphone illustrated in Fig. 10. In this figure, the physical IoT devices are connected to the icons following the steps similar to the standard Bluetooth connection procedure. In BugTalk, pheromone traps and the micro weather stations are connected to the InsectTrap icon (Fig. 10 (1)) and the WeatherSTA icon (Fig. 10 (2)), respectively. When a trap captures a male adult, InsectTrap will receive a signal and increases the number of captured adults. For every hour, InsectTrap sends out the count to the BugTalk server through the input device feature (IDF) Count-I. In Fig. 10, the circles marked Joins 1-7 represent the network programs executed at the BugTalk server, which deliver the data from the IDFs to the output device features (ODFs) connected by these Join links. Similarly, WeatherSTA sends the received temperature and humidity data to the server through Temperature-I and Humidity-I. In the IoTtalk GUI, $M_1$ $(N_F, \boldsymbol{T_n})$ is represented as a cyber IoT device Model1 in two icons: the icon on the right of the window (Fig. 10 (3)) receives $N_F$ through the ODF $N_F$-O and $\boldsymbol{T_n}$ through temperature-O. The Model1 cyber device implements Eq. (1) and the result $N_E$ is sent out from the IDF $N_E$-I in another Model1 icon on the left of the window (Fig. 10 (4)). Similarly, $M_2$ $(N_E, \boldsymbol{T_n}, \boldsymbol{H_n})$ is represented as the cyber IoT device Model2 (Fig. 10 (5) and (6)) that implements Eq. (12), $M_3$ $(N_L, \boldsymbol{T_n})$ is represented as the cyber IoT device Model3 (Fig. 10 (7) and (8)) that implements Eq. (18), and $M_4$ $(N_P, \boldsymbol{T_n})$ is represented as the cyber IoT device Model4 (Fig. 10 (9) and (10)) that computes the final $N_A$ value (Eq. (23)) using Model 4 (Eq. (19)). Note that the ODF humidity-O for Model1, Model3 and Model4 are dummy because the humidity factor has not been included in these models. The final result $N_A$ $(n)$ is produced by Model4 and is shown in the Display device (Fig. 10 (11)) through the Join 7 link (from $N_A$-I to Report-O).

In Fig. 10, the sending end of a join connection is an output of a model (which is an IDF), and the receiving end of the join connection is an input of a model (which is an ODF).

In the Bao farm, InsectTrap and WeatherSTA receive the data from real IoT devices. They can also receive the data from the TARI and CWB databases in the emulation mode.

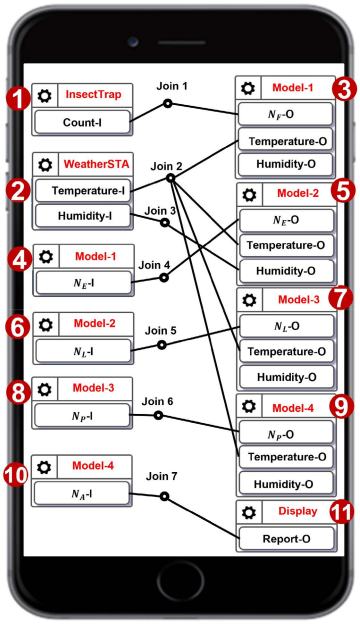


**FIGURE 10.** The BugTalk configuration.

In the latter scenario, BugTalk executes with the timestamps associated with the data instead of the real clock.

Implementation of BugTalk is validated by three tools: BigraphTalk [23], VerificationTalk [24] and SimTalk [25]. BigraphTalk is a verification framework that utilizes formal techniques, based on bigraphs, to statically guarantee that unwanted configurations do not arise. In particular, we check for invalid connections between devices, as well as type errors. VerificationTalk provides IoT functional verification and security check, monitors the flow of data in the system in real time, and eliminates errors and harmful data promptly. SimTalk is a simulation mechanism for correct implementation and behavior investigation.

The ILCYM software is a set of programs used to establish the formulas related to the growth of Spodoptera litura. BugTalk modifies the ILCYM programs to accommodate more accurate temperature and humidity information. The inputs for both ILCYM and BugTalk are the bug numbers accumulated every day. When the TARI dataset is used, we evenly distribute the measured number of 10-day bugs into individual days. The TARI database is connected to the IoTtalk engine through the path (10) in Fig. 8 and the details can be found in [26]. In the current implementation, BugTalk is developed in the IoTtalk platform. We can also implement BugTalk in other service-oriented, scalable and context-aware IoT platforms such as ONTAgriX [27].

In this paper, we use MAAPE to measure the errors of $N_A(n)$ predicted by BugTalk using Eq. (23). MAAPE is modified from MAPE (Mean Absolute Percentage Error) to solve the problem when the denominator of the formula is 0. The MAAPE error is defined as

$$\text{MAAPE} = \left(\frac{100\%}{m}\right) \sum_{n=1}^{m} arctan\left(\left|\frac{N_A^*(n) - N_A(n)}{N_A^*(n)}\right|\right) \tag{24}$$

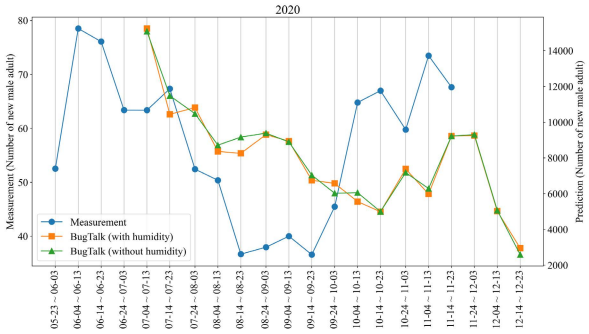


**FIGURE 11.** BugTalk prediction (with and without humidity in Model 2).

**TABLE 4.** Prediction statistics for BugTalk (measurement and scaled prediction in 2020 with 15-day shifting).

| | Measurement | BugTalk |
|---|---|---|
| 05-23~06-03 | 52.532 | - |
| 06-04~06-13 | 78.524 | - |
| 06-14~06-23 | 76.090 | - |
| 06-24~07-03 | 63.393 | - |
| 07-04~07-13 | 63.380 | 73.258 |
| 07-14~07-23 | 67.349 | 60.850 |
| 07-24~08-03 | 52.441 | 73.280 |
| 08-04~08-13 | 50.380 | 59.260 |
| 08-14~08-23 | 36.680 | 66.668 |
| 08-24~09-03 | 37.966 | 62.961 |
| 09-04~09-13 | 40.015 | 48.694 |
| 09-14~09-23 | 36.588 | 44.048 |
| 09-24~10-03 | 45.493 | 42.327 |
| 10-04~10-13 | 64.800 | 37.639 |
| 10-14~10-23 | 66.993 | 50.403 |
| 10-24~11-03 | 59.773 | 60.107 |
| 11-04~11-13 | 73.488 | 72.226 |
| 11-14~11-23 | 67.644 | 52.135 |
| 11-24~12-03 | - | 30.516 |
| 12-04~12-13 | - | 17.143 |
| 12-14~12-23 | - | 2.925 |
| MAAPE | - | 24.593% |

We have conducted the experiments during years 2014-2020. Fig. 11 illustrates the numbers of the new male adults in 2020. The blue circle curve represents the measurements, the orange square curve represents the results of BugTalk considering humidity in Model 2, and the green triangle curve represents the results of BugTalk without considering the humidity. Note that the result of BugTalk is the number of both male and female adults. We divide the

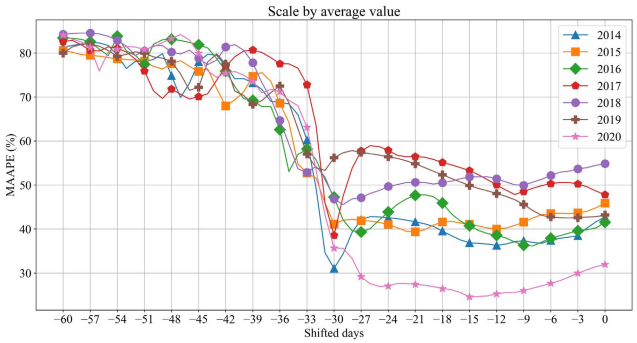


**FIGURE 12.** The shifted MAAPEs.

results by 2 to obtain the number of male adults, and compare it with the measurement. The MAAPE between BugTalk (without humidity) and the measurements is 36.225%, and the MAAPE between BugTalk (with humidity) and the measurements is 35.003%.

Reference [20] used cosine approximation to generate 15-minute temperature predictions. After the cosine approximation in Eqs. (4), (6) and (14), we increase the sampling frequency from one hour per sample to 15 minutes per sample, and the MAAPE performance has been improved. Specifically, the MAAPE between BugTalk (without humidity) and the measurements is 33.478%, and the MAAPE between BugTalk (with humidity) and the measurements is 31.956%.

The figure also indicates that the prediction curves have been ''shifted right'' possibly due to measurement errors. Therefore, we try to shift the prediction curves left for a few days. Fig. 12. illustrates the MAAPEs for the shifted prediction curves during years 2014-2020. The figure indicates that MAAPE decreases and then increases as the number of shifted days increases. The optimal number of the shifted days is less than 30. For example, the optimal MAAPE for 2020 occurs when the curve is shifted left by 15 days, which is 24.593%. Table 4 shows the MAAPE for 15-day shifting. We note that the measurements during 2014-2020 also have measurement errors, and cannot be claimed as ''ground truth''. Fig. 12 shows that the MAAPE performance for year 2020 is better than the previous years due to the improvement of the pheromone trap IoT technology. Details of the pheromone trap IoT technology is out of the scope of this paper and will be addressed in a separate paper.

## VI. CONCLUSION

This paper proposes BugTalk to predict the life of Spodoptera litura (Common Cutworm). Based on IoT, BugTalk is a real-time prediction version of modified ILCYM, an open-source software package that implements the functions used in the four models of the four life stages of Spodoptera litura. We have made the following contributions:

- We have improved the ILCYM functions and several models of the previous studies to increase the accuracy of the prediction.
- We developed the first real-time prediction system that can predict the number of Spodoptera litura for the farm fields in real time. The results are actually compared with the measurements during 2014-2020.
- We have extended the temperature-based ILCYM model to accommodate humidity for the larvae emergence stage, which further improves the accuracy of the model.

The error (MAAPE) between the measurement and the BugTalk prediction is 24.593%. This result has been practically utilized in the farm management, but can be further improved. We note that the measurements are not the ground truth. Therefore, in the future, we will enhance the pheromone trap IoT technology for measurements.

The ILCYM formulas do not consider the humidity condition. From our observation, it is clear that the temperature-only ILCYM model should be enhanced. Therefore, we made the first attempt to include the humidity factor in Model 2 through measurement experiments, which results in a more accurate equation (15). Fig. 11 show that the ILCYM prediction is improved by BugTalk by considering the humidity factor, and such result is consistent with the physical meaning. In the future, we will also conduct experiments to accommodate the humidity factor in Models 1, 3, and 4. By using advanced sensors for real-time data collection, we believe that we have the opportunity to learn more details of the life of Spodoptera litura and provide physical meaning interpretation of the Models 1-4 formulas in the future.

## REFERENCES

[1] R. Tang, F. Liu, Y. Lan, J. Wang, L. Wang, J. Li, X. Liu, Z. Fan, T. Guo, and B. Yue, ''Transcriptomics and metagenomics of common cutworm (*Spodoptera litura*) and fall armyworm (*Spodoptera frugiperda*) demonstrate differences in detoxification and development,'' *BMC Genomics*, vol. 23, no. 1, pp. 1–15, Dec. 2022, doi: 10.1186/s12864-022-08613-6.

[2] L. Tian, X. Gao, S. Zhang, Y. Zhang, D. Ma, and J. Cui, ''Dynamic changes of transcriptome of fifth-instar *Spodoptera litura* larvae in response to insecticide,'' *3 Biotech*, vol. 11, no. 2, pp. 1–12, Feb. 2021, doi: 10.1007/s13205-021-02651-9.

[3] C. Bragard, ''Pest categorisation of *Spodoptera litura*,'' *EFSA J.*, vol. 17, no. 7, pp. 1–12, Jul. 2019, doi: 10.2903/j.efsa.2019.5765.

[4] G. V. R. Rao, J. A. Wightman, and D. V. R. Rao, ''Threshold temperatures and thermal requirements for the development of *Spodoptera litura* (Lepidoptera: Noctuidae),'' *Environ. Entomol.*, vol. 18, no. 4, pp. 548–551, Aug. 1989, doi: 10.1093/ee/18.4.548.

[5] S.-J. Tuan, C.-C. Lee, and H. Chi, ''Population and damage projection of *Spodoptera litura* (F.) on peanuts (*Arachis hypogaea* L.) under different conditions using the age-stage, two-sex life table,'' *Pest Manage. Sci.*, vol. 70, no. 5, pp. 805–813, May 2014, doi: 10.1002/ps.3618.

[6] C. N. Rao and A. George, ''Tobacco caterpillar, *Spodoptera litura* Fabricius (Noctuidae: Lepidoptera),'' in *Pests Their Management*. Singapore: Springer, 2018, pp. 179–180.

[7] M. Sporleder, D. Chavez, J. C. Gonzales, H. Juarez, R. Simon, and J. Kroschel, ''ILCYM-Insect life cycle modeling: Software for developing temperature-based insect phenology models with applications for regional and global pest risk assessments and mapping,'' in *Proc. 15th Triennial ISTRC Symp. Int. Soc. Tropical Root Crops (ISTRC)*. Lima, Peru, 2009, pp. 216–223.

[8] Y.-B. Lin, Y.-W. Lin, C.-M. Huang, C.-Y. Chih, and P. Lin, ''IoTtalk: A management platform for reconfigurable sensor devices,'' *IEEE Internet Things J.*, vol. 4, no. 5, pp. 1152–1562, Oct. 2017, doi: 10.1109/JIOT.2017.2682100.

[9] S. R. Babu, R. K. Kalyan, G. S. Ameta, and M. L. Meghwal, "Analysis of outbreak of tobacco caterpillar, *Spodoptera litura* (Fabricius) on soybean," *J. Agrometeorol.*, vol. 17, no. 1, pp. 61–66, Jun. 2015, doi: 10.54386/jam.v17i1.987.

[10] S. Vennila, G. Singh, G. K. Jha, M. S. Rao, H. Panwar, and M. Hegde, "Artificial neural network techniques for predicting severity of *Spodoptera litura* (Fabricius) on groundnut," *J. Environ. Biol.*, vol. 38, no. 3, pp. 449–456, May 2017, doi: 10.22438/jeb/38/3/ms-163.

[11] P. Duraimurugan, "Effect of weather parameters on the seasonal dynamics of tobacco caterpillar, *Spodoptera litura* (Lepidoptera: Noctuidae) in castor in telangana state," *J. Agrometeorol.*, vol. 20, no. 2, pp. 139–143, Dec. 2021, doi: 10.54386/jam.v20i2.526.

[12] A. A. Tompe, U. B. Hole, S. R. Kulkarni, C. S. Chaudhari, and S. K. Chavan, "Studies on seasonal incidence of leaf eating caterpillar, *Spodoptera litura* (Fab.) infesting capsicum under polyhouse condition," *SAARC J. Entomol. Zool. Stud.*, vol. 8, no. 1, pp. 761–764, 2020.

[13] M. Khan and S. Talukder, "Influence of weather factors on the abundance and population dynamics of *Spodoptera litura* F. And Pieris brassicae L. On cabbage," *SAARC J. Agricult.*, vol. 15, no. 1, pp. 13–21, Jul. 2017, doi: 10.3329/sja.v15i1.33147.

[14] G. L. Curry, R. M. Feldman, and K. C. Smith, "A stochastic model of a temperature-dependent population," *Theor. Population Biol.*, vol. 13, no. 2, pp. 197–213, 1978, doi: 10.1016/0040-5809(78)90042-4.

[15] D.-S. Kim, J.-H. Lee, and M.-S. Yiem, "Temperature-dependent development of *Carposina sasakii* (Lepidoptera: Carposinidae) and its stage emergence models," *Environ. Entomol.*, vol. 30, no. 2, pp. 298–305, Apr. 2001, doi: 10.1603/0046-225X-30.2.298.

[16] D.-S. Kim and and J.-H. Lee, "Oviposition model of *Carposina sasakii* (Lepidoptera: Carposinidae)," *Ecol. Model.*, vol. 162, nos. 1–2, pp. 145–153, 2003, doi: 10.1016/S0304-3800(02)00402-7.

[17] P. Hardik and K. Dolly, "Effect of abiotic factors on the life cycle of *Spodoptera litura* Fabricius, 1775 (Lepidoptera: Noctuidae)," *Appl. Ecol. Environ. Sci.*, vol. 8, no. 3, pp. 87–91, 2020.

[18] H. Colinet, "Disruption of ATP homeostasis during chronic cold stress and recovery in the chill susceptible beetle (Alphitobius diaperinus)," *Comparative Biochemistry Physiol. A, Mol. Integrative Physiol.*, vol. 160, no. 1, pp. 63–67, Sep. 2011, doi: 10.1016/j.cbpa.2011.05.003.

[19] W. Zhu, H. Zhang, Q. Meng, M. Wang, G. Zhou, X. Li, H. Wang, L. Miao, Q. Qin, and J. Zhang, "Metabolic insights into the cold survival strategy and overwintering of the common cutworm, *Spodoptera litura* (Fabricius) (lepidoptera: Noctuidae)," *J. Insect Physiol.*, vol. 100, pp. 53–64, Jul. 2017, doi: 10.1016/j.jinsphys.2017.05.008.

[20] B. B. Fand, N. T. Sul, S. K. Bal, and P. S. Minhas, "Temperature impacts the development and survival of common cutworm (*Spodoptera litura*): Simulation and visualization of potential population growth in India under warmer temperatures through life cycle modelling and spatial mapping," *PLoS ONE*, vol. 10, no. 4, Apr. 2015, Art. no. e0124682, doi: 10.1371/journal.pone.0124682.

[21] R. M. Schoolfield, P. J. H. Sharpe, and C. E. Magnuson, "Non-linear regression of biological temperature-dependent rate models based on absolute reaction-rate theory," *J. Theor. Biol.*, vol. 81, pp. 719–731, Feb. 1981, doi: 10.1016/0022-5193(81)90246-0.

[22] W.-L. Chen, Y.-B. Lin, Y.-W. Lin, R. Chen, J.-K. Liao, F.-L. Ng, Y.-Y. Chan, Y.-C. Liu, C.-C. Wang, C.-H. Chiu, and T.-H. Yen, "AgriTalk: IoT for precision soil farming of turmeric cultivation," *IEEE Internet Things J.*, vol. 6, no. 3, pp. 5209–5223, Jun. 2019, doi: 10.1109/JIOT.2019.2899128.

[23] B. Archibald, M.-Z. Shieh, Y.-H. Hu, M. Sevegnani, and Y.-B. Lin, "BigraphTalk: Verified design of IoT applications," *IEEE Internet Things J.*, vol. 7, no. 4, pp. 2955–2967, Apr. 2020, doi: 10.1109/JIOT.2020.2964026.

[24] M.-Z. Shieh, Y.-B. Lin, and Y.-J. Hsu, "VerificationTalk: A verification and security mechanism for IoT applications," *Sensors*, vol. 21, no. 22, p. 7449, Nov. 2021, doi: 10.3390/s21227449.

[25] Y.-W. Lin, Y.-B. Lin, and T.-H. Yen, "SimTalk: Simulation of IoT applications," *Sensors*, vol. 20, no. 9, p. 2563, Apr. 2020, doi: 10.3390/s20092563.

[26] Y.-W. Lin, Y.-B. Lin, C.-Y. Liu, J.-Y. Lin, and Y.-L. Shih, "Implementing AI as cyber IoT devices: The house valuation example," *IEEE Trans. Ind. Informat.*, vol. 16, no. 4, pp. 2612–2620, Apr. 2020, doi: 10.1109/TII.2019.2951847.

[27] M. Fahad, T. Javid, H. Beenish, A. A. Siddiqui, and G. Ahmed, "Extending ONTAgri with service-oriented architecture towards precision farming application," *Sustainability*, vol. 13, no. 17, p. 9801, Aug. 2021, doi: 10.3390/su13179801.


**LI-XIAN CHEN** received the B.S. degree in computer science and information engineering from the National Ilan University, Yilan City, Taiwan, in 2020. He is currently pursuing the M.S. degree with the Institute of Network Engineering, National Yang Ming Chiao Tung University, Hsinchu City, Taiwan. His current research interests include the Internet of Things and machine learning.

**WEN-LIANG CHEN** received the Ph.D. degree in biotechnology from the National Chiao Tung University, Hsinchu, Taiwan, in 2006. He joined the National Yang Ming Chiao Tung University, in 2008, where he is currently a Professor with the Department of Biological Science and Technology. His research interests include protein chemistry, protein engineering, synthetic biology, cancer biology, antibody engineering, and development of biomaterial-based drug repositioning platforms for cancer treatment.

**MING-YAO CHIANG** received the M.S. degree in entomology from the National Chung-Hing University, Taichung, Taiwan, in 1998. He is currently an Assistant Researcher Fellow with the Taiwan Agricultural Research Institute, Taichung. His current research interests include rapid bioassay for pesticide residues, insecticide resistance, pest attractant, and pest IPM research.

**YI-BING LIN** (Fellow, IEEE) received the Ph.D. degree in computer science from the University of Washington, Seattle, USA, in 1990. He is currently the Winbond Chair Professor of the National Yang Ming Chiao Tung University (NYCU), the Chair Professor of the National Cheng Kung University and China Medical University, and an Adjunct Research Fellow of Academia Sinica. From 1990 to 1995, he was a Research Scientist with Bellcore. Then, he joined NCTU, and became a Senior Vice President of NCTU, in 2011. During 2014 to 2016, he was a Deputy Minister of the Ministry of Science and Technology, Taiwan. He is the coauthor of the books *Wireless and Mobile Network Architecture* (Wiley, 2001), *Wireless and Mobile All-IP Networks* (John Wiley, 2005), and *Charging for Mobile All-IP Telecommunications* (Wiley, 2008). He is a fellow of AAAS, ACM, and IET.

**YUN-WEI LIN** (Member, IEEE) received the Ph.D. degree in computer science and information engineering from the National Chung Cheng University, Chiayi, Taiwan, in 2011. He has been an Associate Professor with the College of Artificial Intelligence, National Chiao Tung University, Hsinchu, Taiwan, since 2021. His current research interests include mobile *ad-hoc* networks, wireless sensor networks, vehicular *ad hoc* networks, and the IoT/M2M communications.

**FUNG-LING NG** received the B.S. degree in biological science and technology from the National Chiao Tung University, Taiwan, in 2017. She is currently pursuing the Ph.D. degree in biological science and technology. Her current research interests include bio-pesticides application and precision farming management.